Supplement of Atmos. Chem. Phys., 26, 14699–14723, 2026
https://doi.org/10.5194/acp-26-14699-2026-supplement
© Author(s) 2026. CC BY 4.0 License.

Atmospheric Chemistry and Physics
Open Access

Supplement of

Can radon help to improve methane emission estimates? Results from a dual-tracer inversion

Fabian Maier et al.

Correspondence to: Fabian Maier (fmaier@bgc-jena.mpg.de)

The copyright of individual parts of the supplement might differ from the article licence.

Supplement

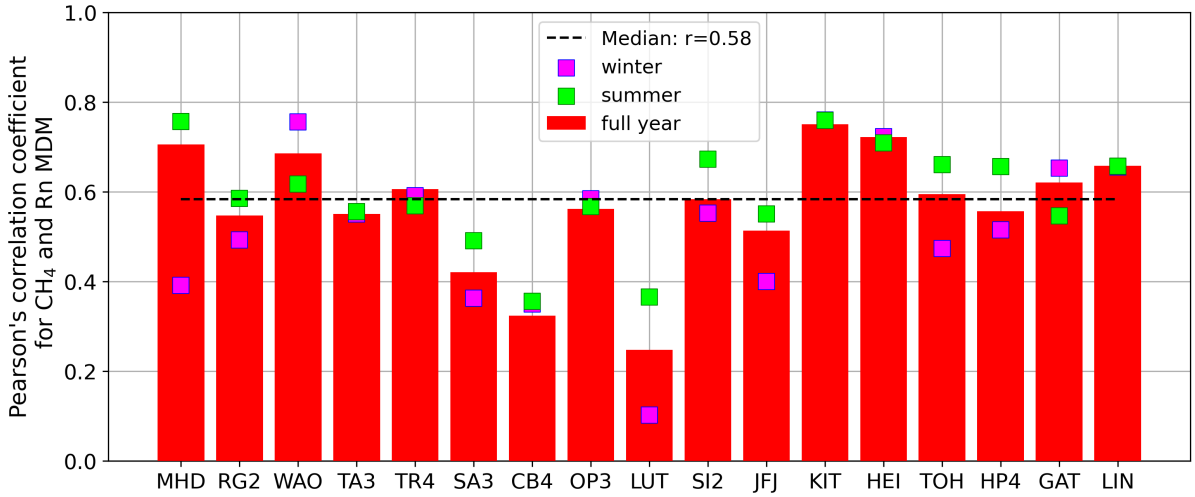

Figure S1: Pearson's correlation coefficient for the 3σ-outlier flagged afternoon (and night-time, respectively, for mountain sites) CH_4 and Rn MDM of all 17 observations sites in 2021. The red bars show the correlation coefficient for the full year 2021, and the magenta and green squares for the winter and summer half-year 2021, respectively. The median correlation coefficient is given by the dashed black line.

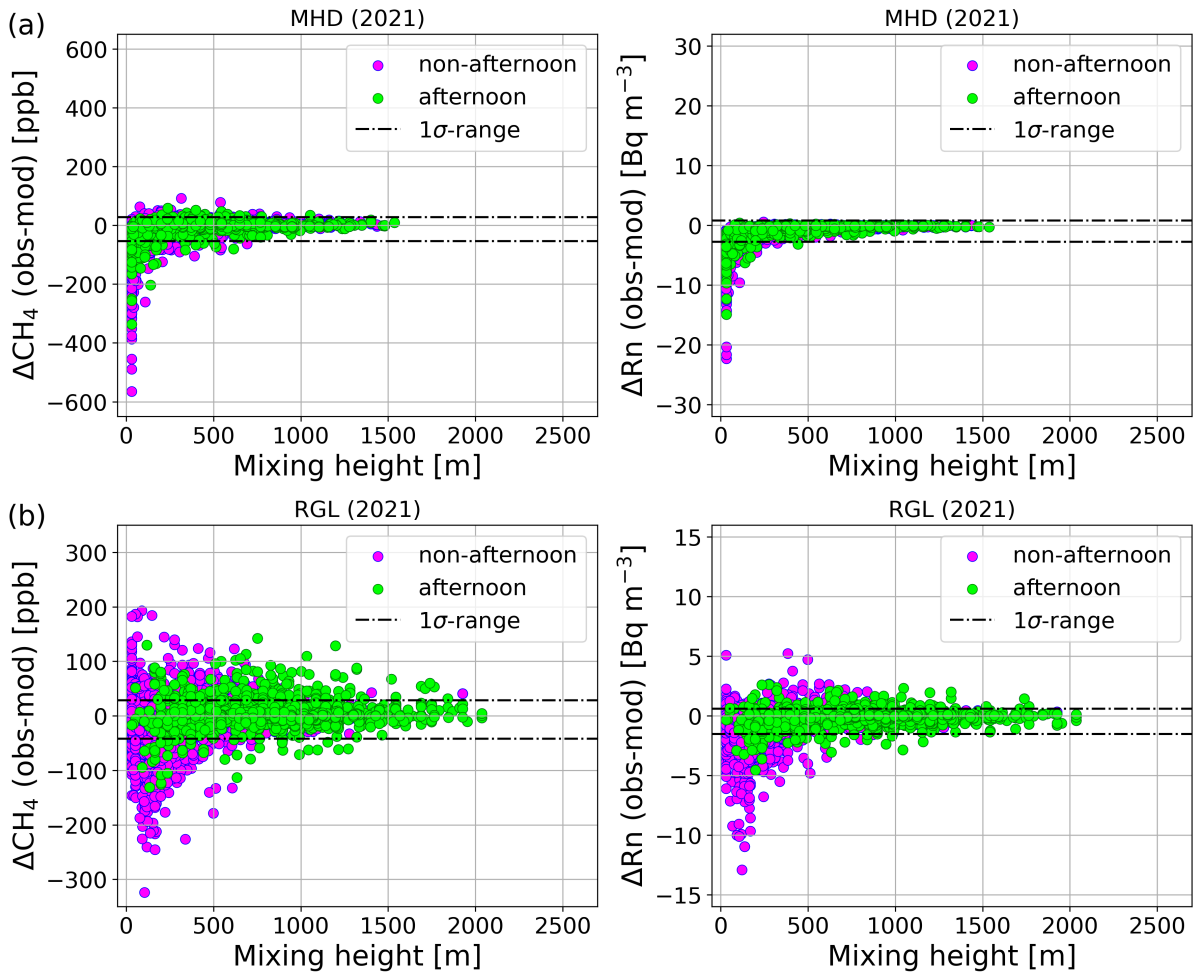

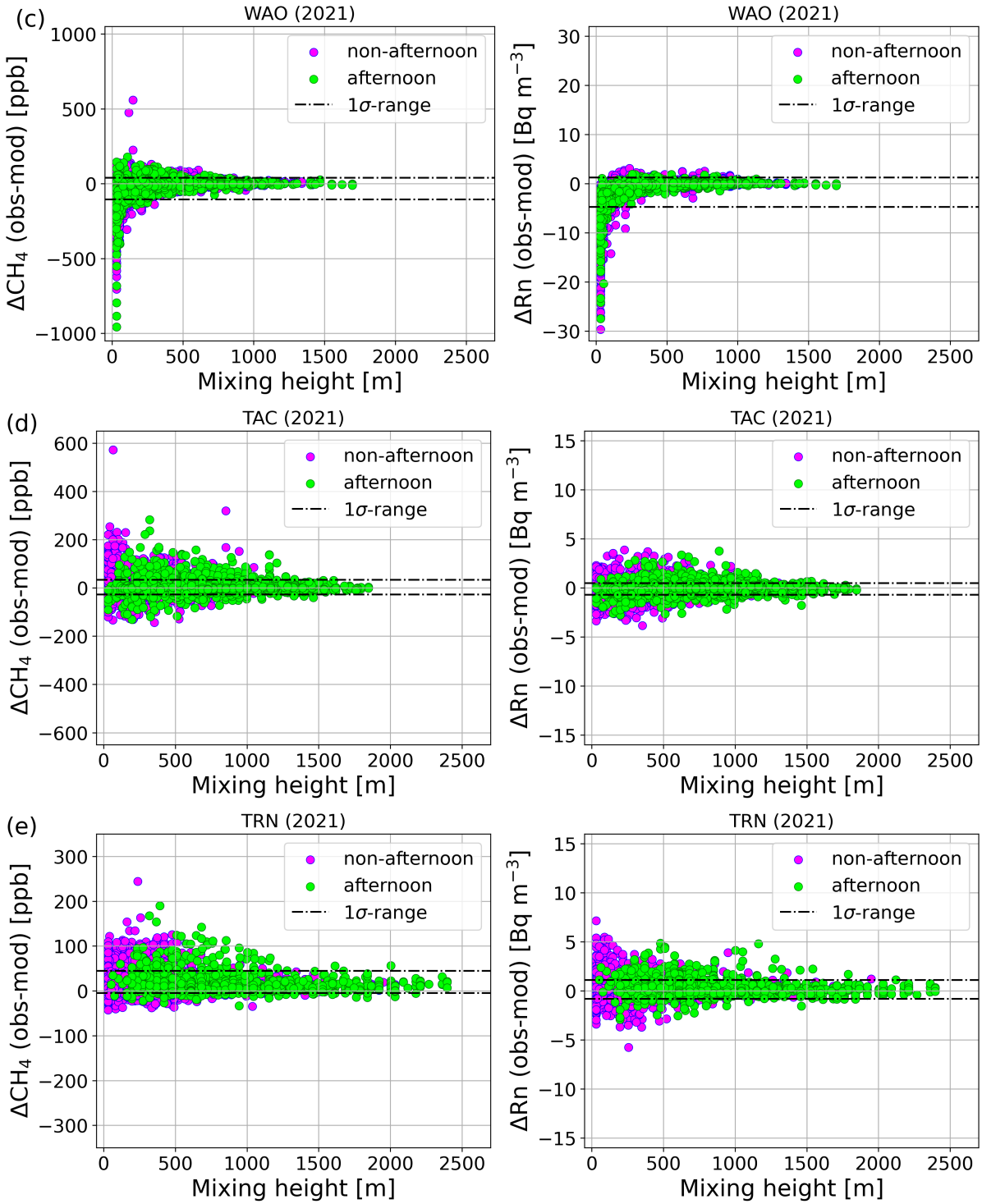
(c)
WAO (2021)
non-afternoon
afternoon
1σ-range
ΔCH4 (obs-mod) [ppb]
ΔRn (obs-mod) [Bq m−3]
Mixing height [m]
(d)
TAC (2021)
(e)
TRN (2021)

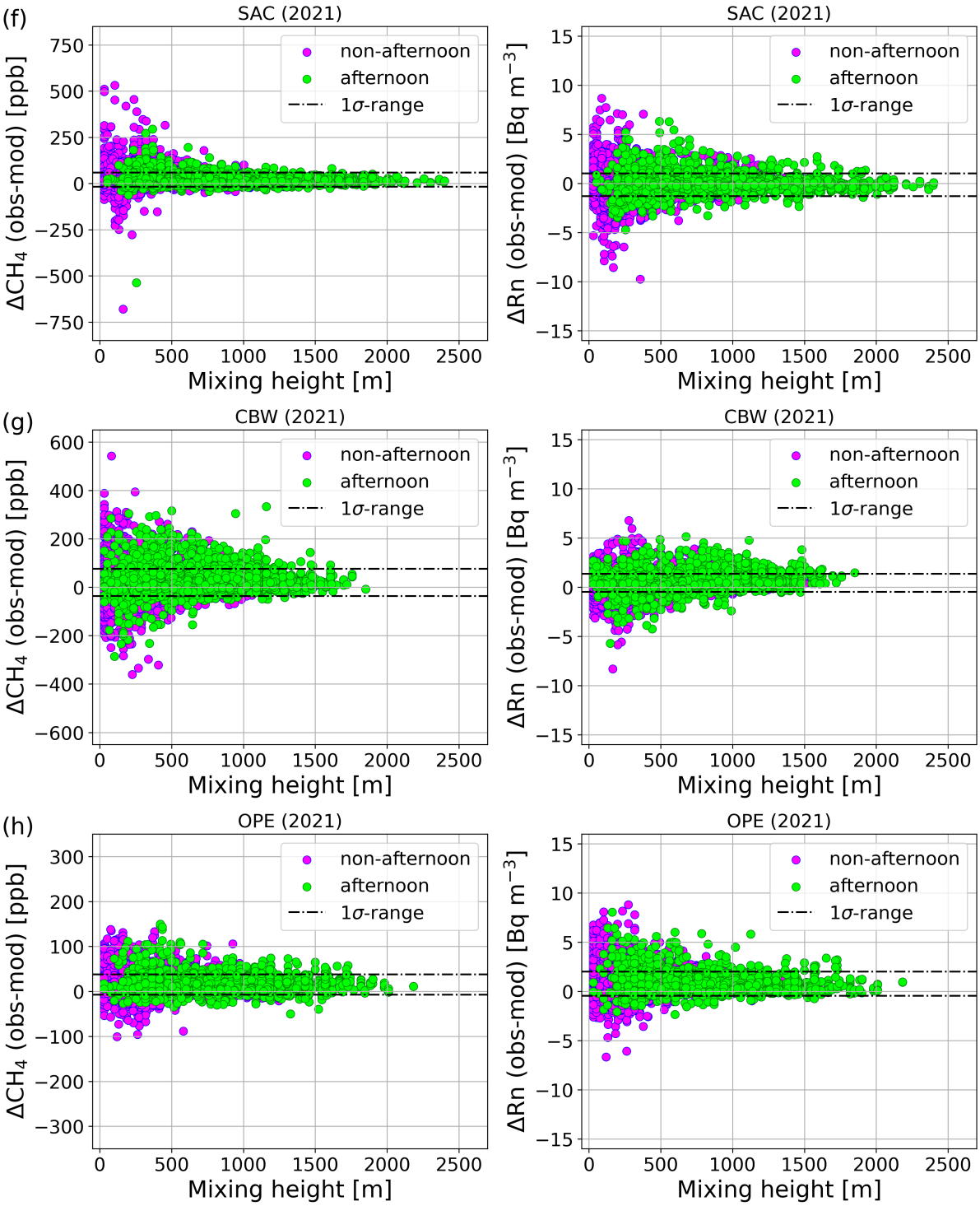
(f)
SAC (2021)
non-afternoon
afternoon
1σ-range
ΔCH4 (obs-mod) [ppb]
ΔRn (obs-mod) [Bq m−3]
Mixing height [m]
(g)
CBW (2021)
(h)
OPE (2021)

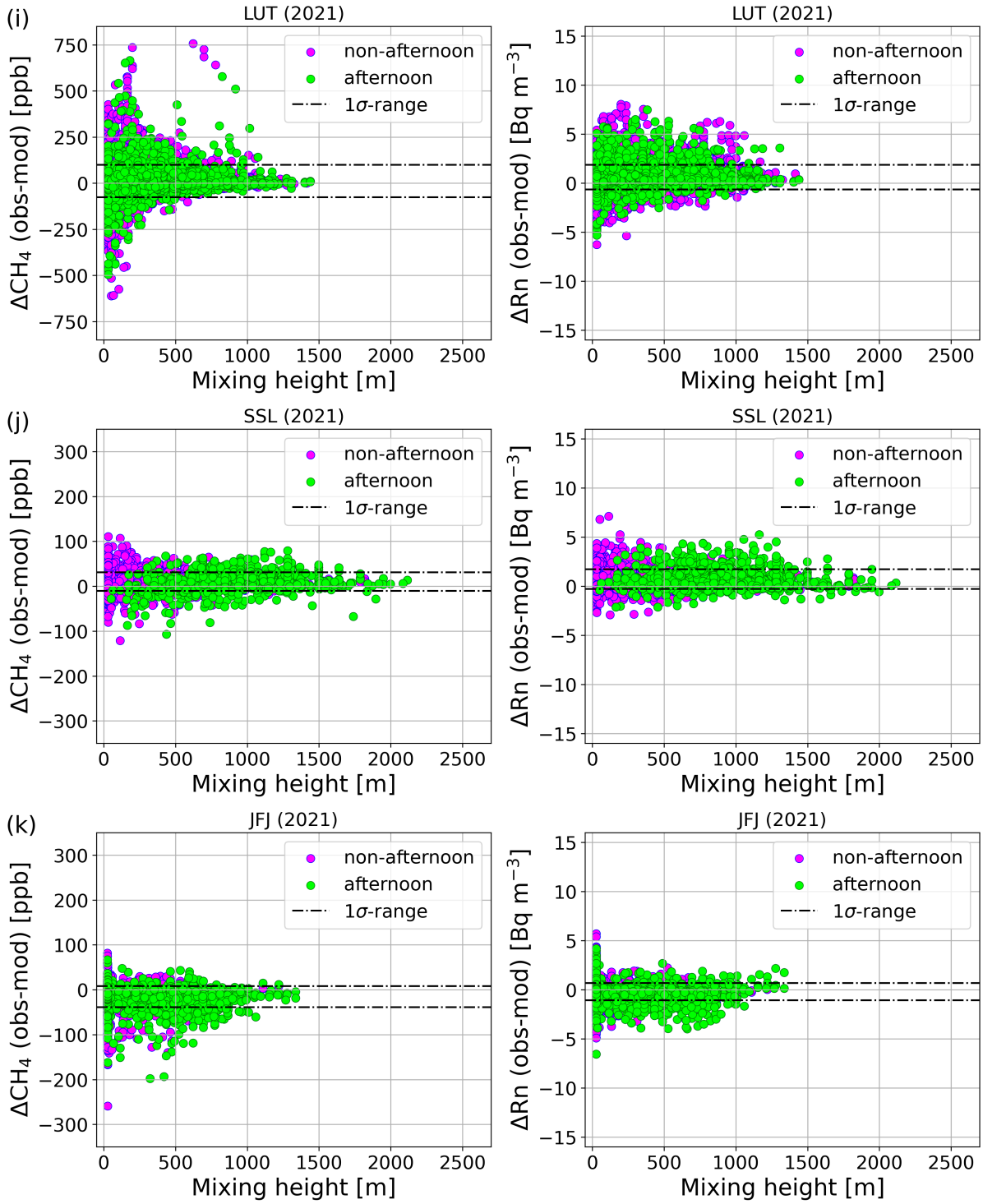
(i)
LUT (2021)
non-afternoon
afternoon
1σ-range
ΔCH4 (obs-mod) [ppb]
ΔRn (obs-mod) [Bq m−3]
Mixing height [m]
(j)
SSL (2021)
(k)
JFJ (2021)

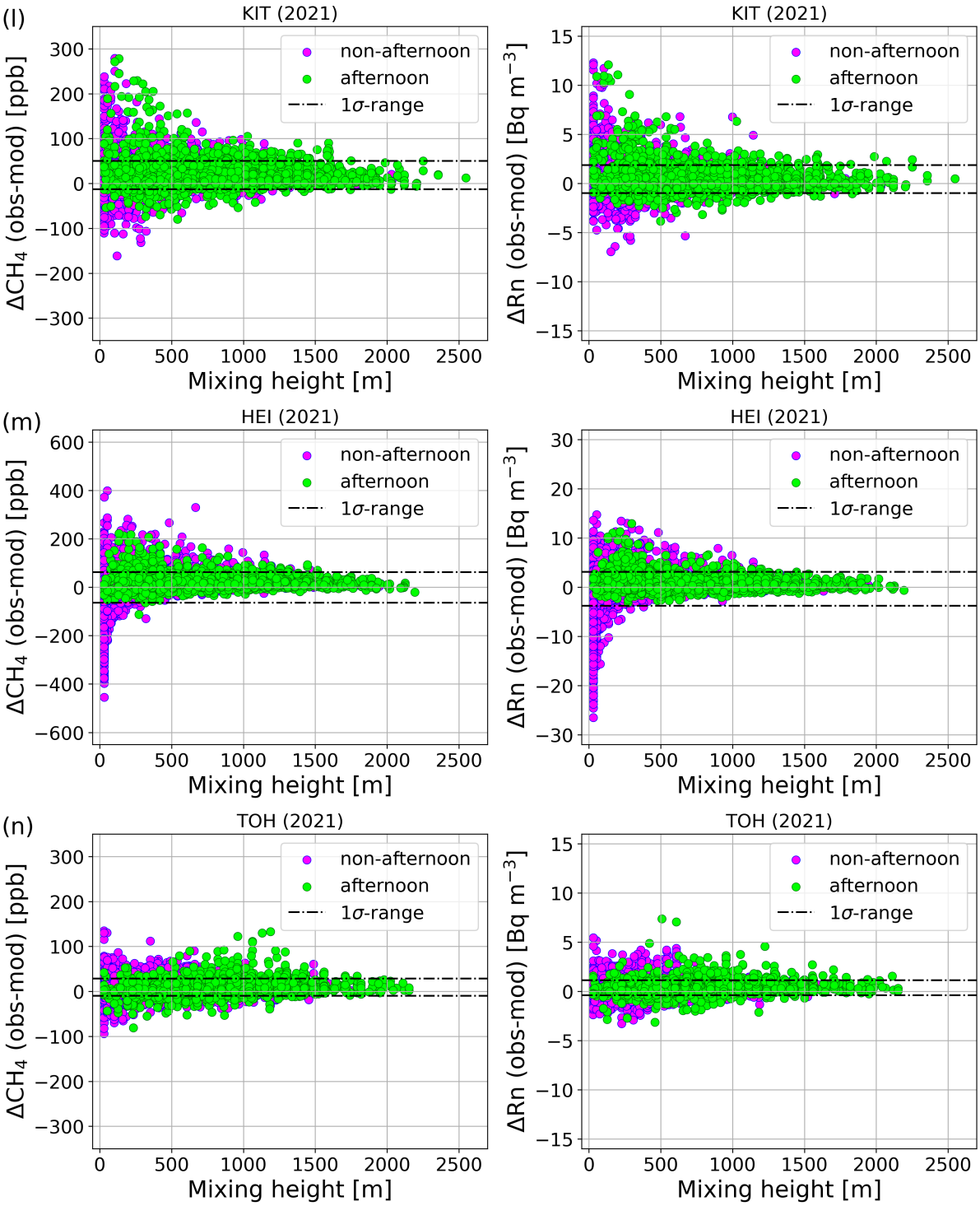
(l)
KIT (2021)
non-afternoon
afternoon
1σ-range
ΔCH4 (obs-mod) [ppb]
Mixing height [m]
KIT (2021)
ΔRn (obs-mod) [Bq m−3]
Mixing height [m]
(m)
HEI (2021)
ΔCH4 (obs-mod) [ppb]
Mixing height [m]
HEI (2021)
ΔRn (obs-mod) [Bq m−3]
Mixing height [m]
(n)
TOH (2021)
ΔCH4 (obs-mod) [ppb]
Mixing height [m]
TOH (2021)
ΔRn (obs-mod) [Bq m−3]
Mixing height [m]

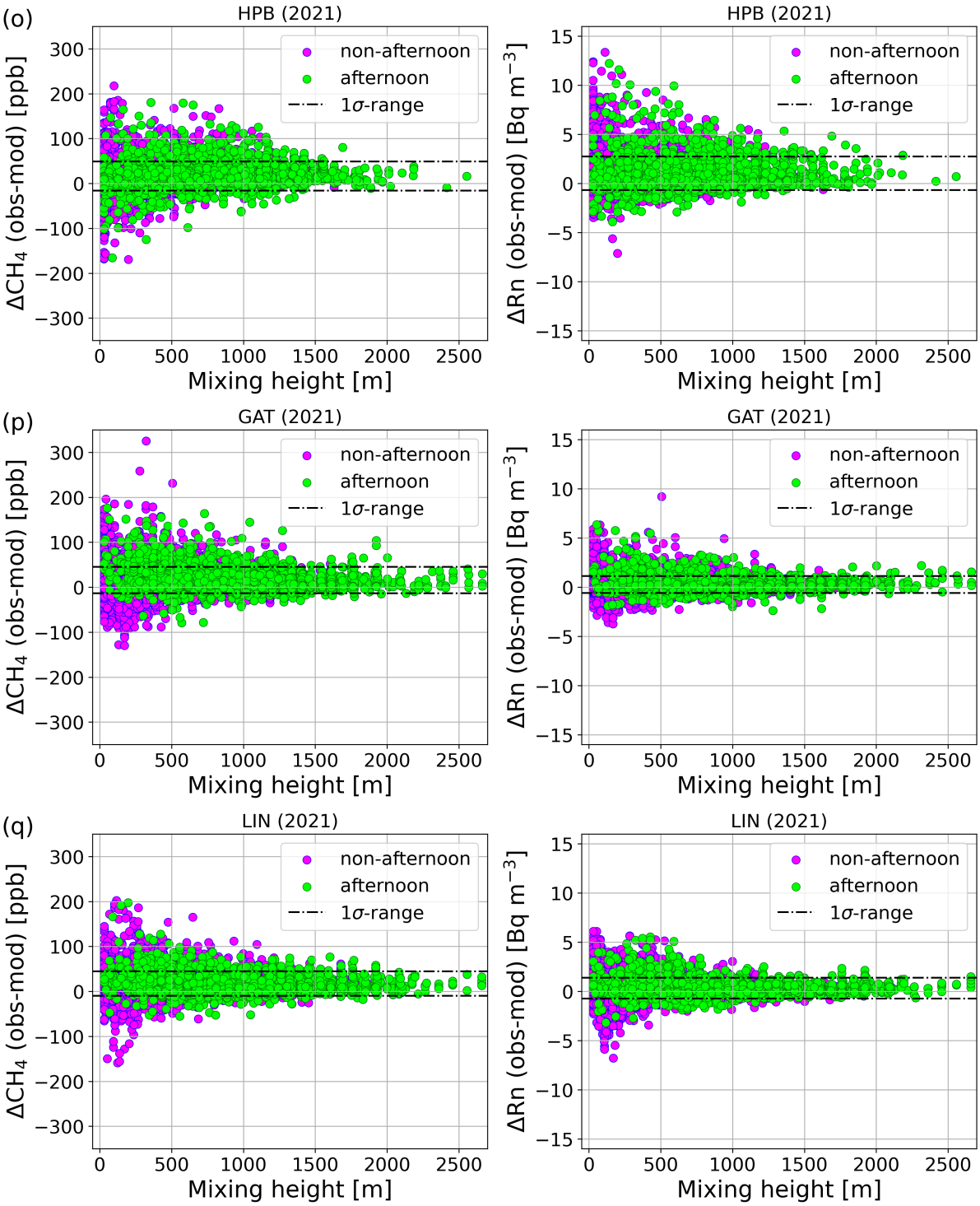

Figure S2: Hourly CH_4 (left panels) and Rn (right panels) MDM in dependence of the modelled mixing height from STILT for all 17 European observation sites, ordered from west (a) to east (q). Afternoon (11-16 UTC) data and non-afternoon data are shown in green and magenta, respectively. The standard deviation (1σ-range) of the CH_4 and Rn MDM (afternoon and non-afternoon data) is indicated by the dashed black lines.

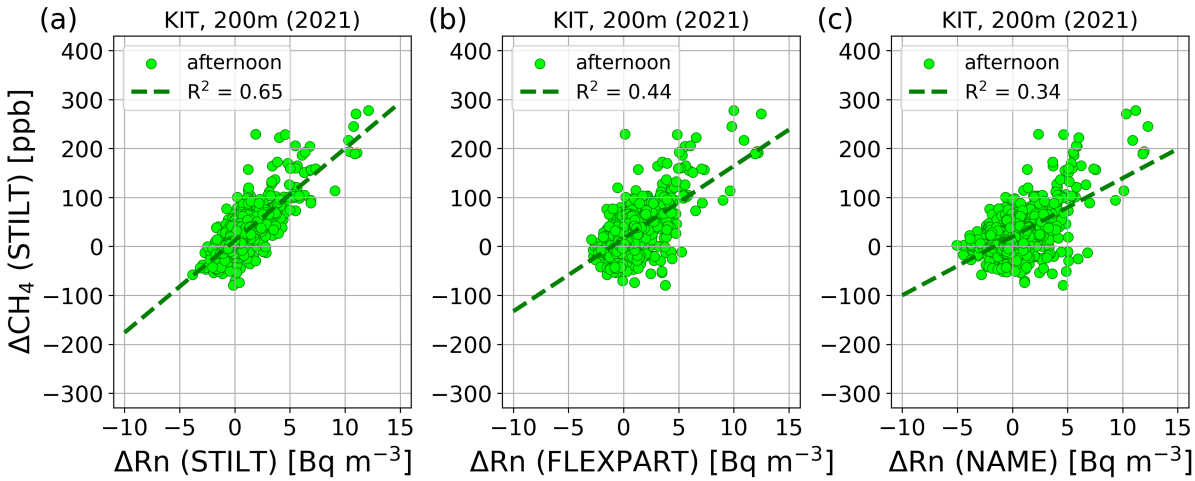

Figure S3: Correlation between the hourly CH_4 MDM (observed minus modelled CH_4 concentration) based on STILT simulations and (a) the Rn MDM based on STILT simulations, (b) the Rn MDM based on FLEXPART simulations, and (c) the Rn MDM based on NAME simulations. Shown are the results for afternoon observations in 2021 from the Karlsruhe (KIT) tower site (200 m agl). The dashed line shows a linear regression through the data.

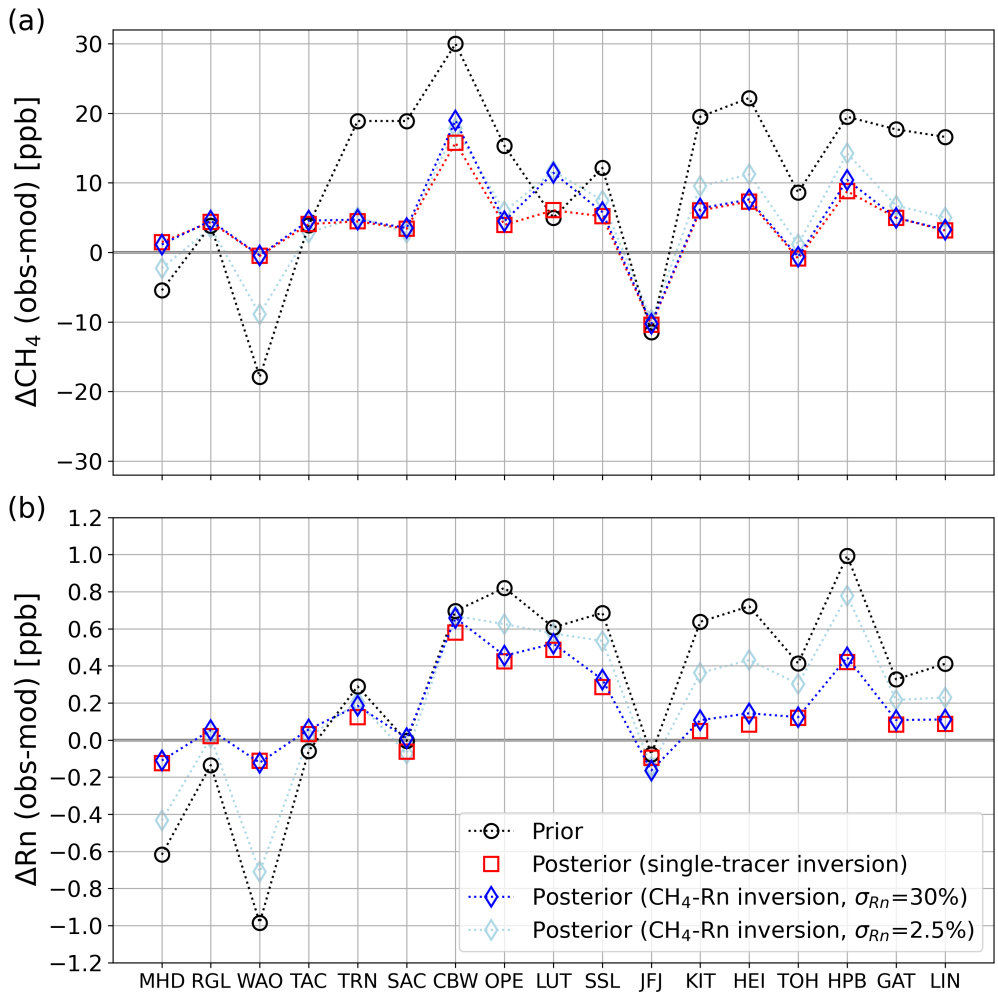

Figure S4: Annual mean CH_4 (a) and Rn (b) MDMs (i.e. differences between observed and modelled concentrations) for each observation site. The MDMs were calculated using the prior fluxes (black), the posterior fluxes from the single-tracer inversions (red), the posterior fluxes from the dual-tracer inversion with the standard Rn prior flux uncertainty of 30% for the annual total flux of the full European model domain (dark blue), and the (unrealistic) extreme case with a reduced Rn prior flux uncertainty of 2.5% (light blue). The latter is shown only to illustrate the effect of the Rn information on the CH_4 posterior MDM. The observation sites are ordered from west (left) to east (right).

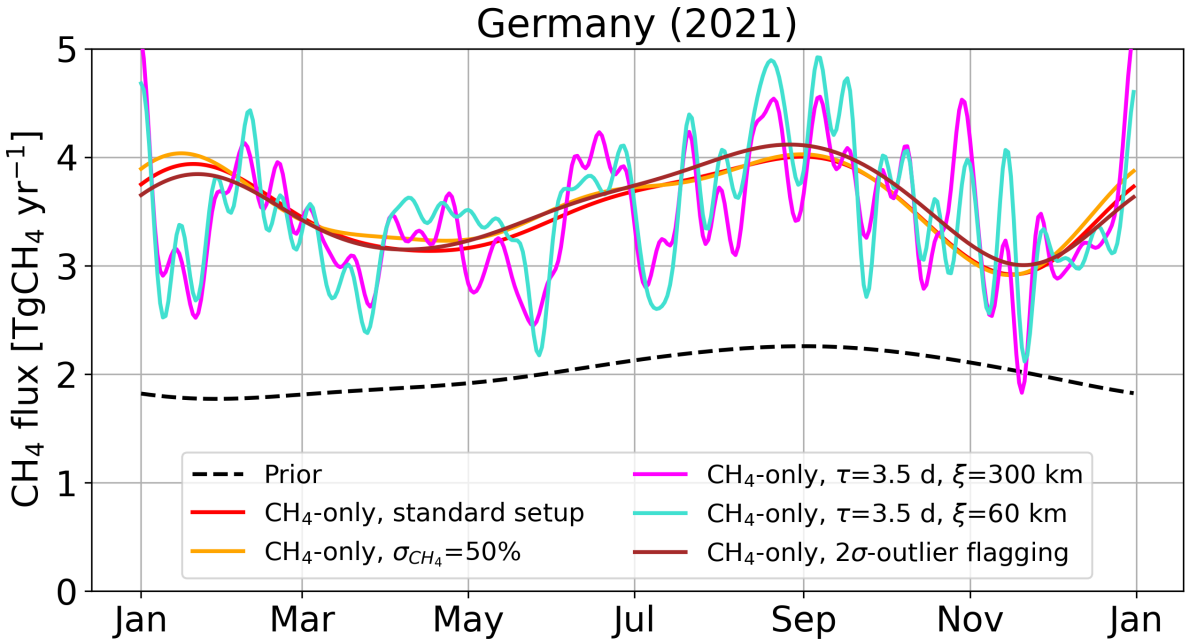

Figure S5: Robustness of the CH_4-only inversion results for Germany in 2021. Shown are the posterior fluxes for the standard configuration described in Sect. 2.2 (red), for 50% (instead of 30%) prior flux uncertainty for the annual total flux of the European model domain (orange), for a reduced temporal correlation length τ of 3.5 days (instead of 1 month; magenta), for a reduced temporal (τ) and spatial (ξ) correlation length of 3.5 days and 60 km, respectively (turquoise), and for a 2σ- (instead of 3σ-) outlier flagged data set. All results are based on the same prior flux (black dashed line).

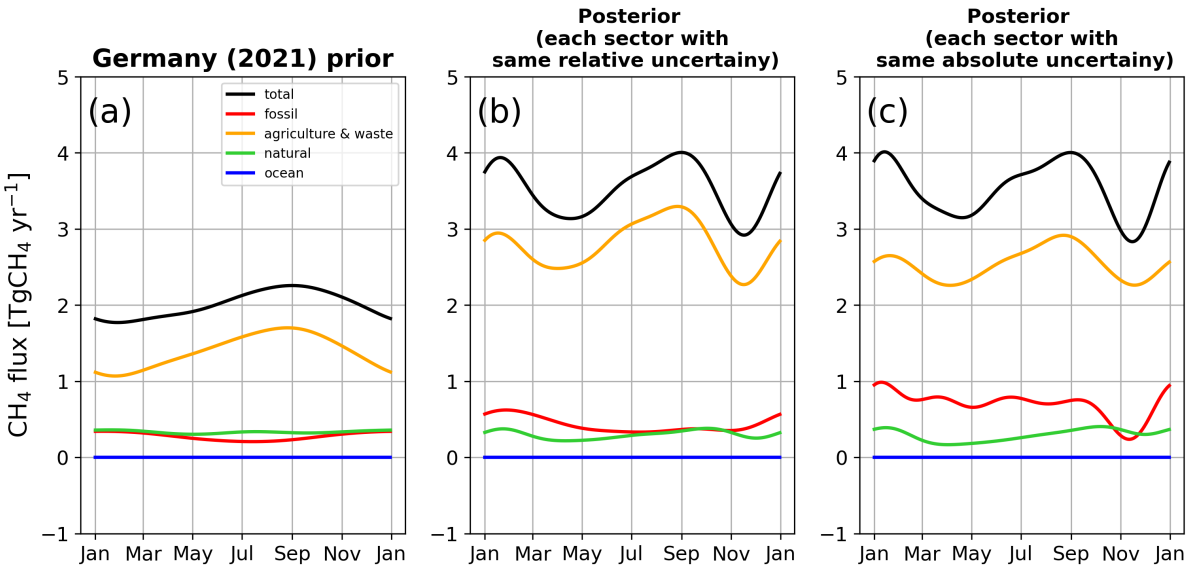

Figure S6: Single-tracer inversion estimates of CH_4 fluxes for Germany, by sector (colored curves), for (a) the prior fluxes, (b) the posterior fluxes from the standard inversion configuration with equal relative prior flux uncertainties across sectors, and (c) the posterior fluxes from an alternative inversion with equal absolute prior flux uncertainties across sectors. In panel (c), an absolute prior flux uncertainty of 30% of the European total prior flux from the agriculture and waste sector (orange) was applied uniformly to all sectors.

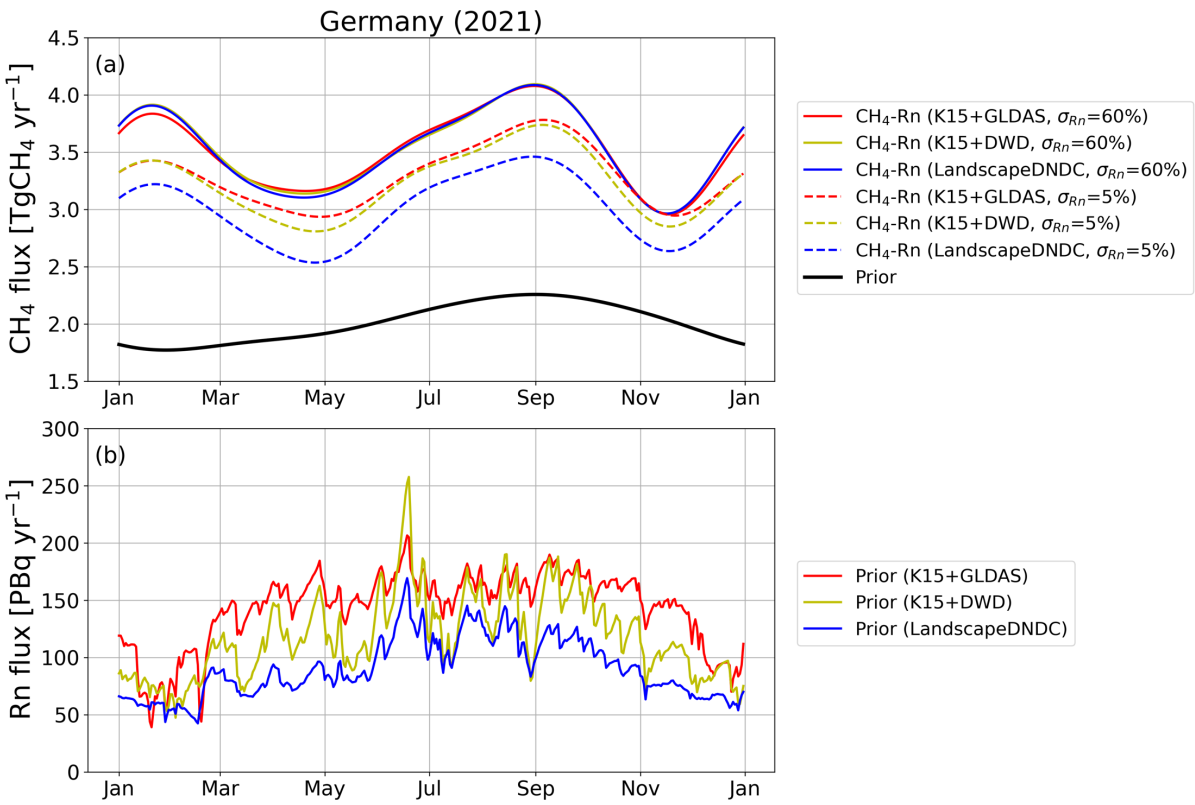

Figure S7: Dual-tracer estimates of CH_4 fluxes for Germany based on three different Rn prior flux estimates. Panel (a) shows the different CH_4 flux estimates under two uncertainty assumptions for the Rn prior flux: 60% (coloured solid curves) and unrealistic 5% (coloured dashed curves). Panel (b) displays the three distinct Rn prior flux estimates used in the dual-tracer approach. For a description of the Rn prior flux estimates, refer to Sect. 2.1.3 and Tab. 2 in the manuscript.

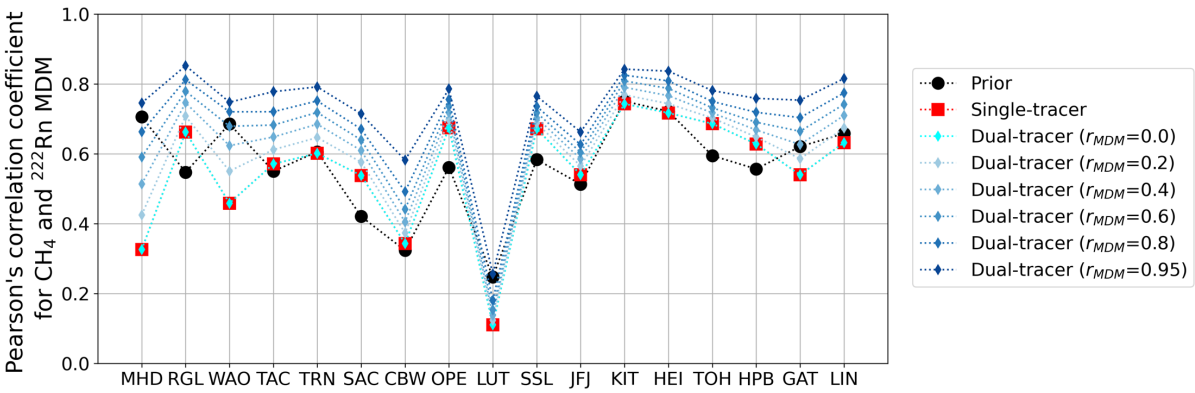

Figure S8: Prior (black) and posterior CH_4-Rn MDM correlation coefficients for the single-tracer (red) and different dual-tracer runs (bluish curves) based on different r_{MDM} values set in the MDM error covariance matrix. Shown are the correlation coefficients for the full year 2021 for each site.

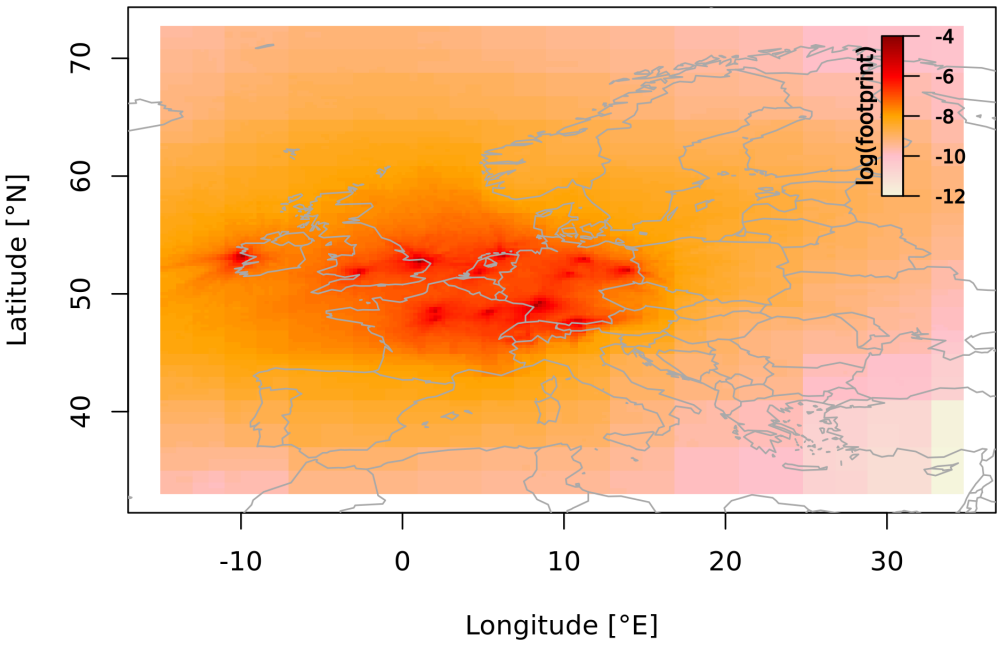

Figure S9: Average footprint of the 17 sites used in the inversion for 2021. The average footprint is shown on a logarithmic scale and is expressed in units of ppm/(µmol $m^{-2}s^{-1}$).